View metadata, citation and similar papers at core.ac.uk
brought to you by CORE
provided by National Tsing Hua University Institutional Repository

Transport, magnetic, specific heat, internal friction, and shear modulus in the charge ordered $La_{0.25}Ca_{0.75}MnO_3$ manganite

R. K. Zheng, A. N. Tang, Y. Yang, W. Wang, G. Li, and X. G. Li[a)]
Structure Research Laboratory, Department of Materials Science and Engineering, University of Science and Technology of China, Anhui, Hefei 230026, China

H. C. Ku
Department of Physics, The National Tsing Hua University, Hsinchu 300, Taiwan, China

(Received 16 December 2002; accepted 28 April 2003)

The resistivity, magnetization, specific heat, shear modulus, and internal friction in the charge-ordered (CO) $La_{0.25}Ca_{0.75}MnO_3$ were studied. The electronic conduction in the CO state was found to obey Mott's variable-range hopping model with a change in the localization length ξ near T_N. A large decrease of the magnetization was observed between the Néer temperature T_N and the charge ordering transition temperature T_{CO}, which was attributed to the consequence of the orbital ordering. Drastic stiffening in shear modulus and an internal friction peak appeared just below T_{CO}, and were explained as due to the coupling between the lattice strain and the orbital degree of freedom. A small upturn of the magnetization and a small softening of the ultrasound near $T_{CA} \approx 42$ K suggest the evolution of spin canting from the matrix of long-range antiferromagnetic state.
© *2003 American Institute of Physics.* [DOI: 10.1063/1.1583150]

I. INTRODUCTION

The charge ordering (CO) phenomena, characterized by an ordering of the Mn^{3+} and Mn^{4+} species within the MnO_2 plane, in hole-doped perovskite-type manganites $R_{1-x}A_xMnO_3$ (where R and A are trivalent rare-earth and divalent alkaline-earth ions, respectively) have recently attracted much attention because of their rich electronic, magnetic, and structural phase diagrams.[1–3] In particular, the $La_{1-x}Ca_xMnO_3$ system, in the doping range of $0.5 \leqslant x \leqslant 0.875$, undergoes charge, spin, and orbital ordering phase transitions, as well as a large change of the lattice parameters upon cooling below the charge ordering transition temperature T_{CO}.[4–6] For $x=0.5$, the compound first undergoes a paramagnetic to ferromagnetic transition at about $T_C \approx 225$ K on cooling.[7] With further cooling of temperature from T_C, it shows an unpredicted coexistence of ferromagnetic metallic and incommensurate charge ordering insulator clusters,[8] and ferromagnetic metallic and incommensurate charge ordering transition at $T_N \approx 155$ K.[7] The magnetic structure in the CO state for $x=0.5$ is CE type which is built up of the coherent stacking of octants of the C-type and E-type magnetic structures.[9] With increasing x from 0.5 to 0.75 the CO state becomes increasingly stable,[10] and the magnetic structure evolves from CE type to C type. At the same time, the effective electron-lattice interaction with the cooperative Jahn–Teller distortion increases, and hence the phase separation tendency was suppressed.[10] Recent ultrasound studies on $La_{1-x}Ca_xMnO_3$ ($0.5 \leqslant x \leqslant 0.87$) show that the cooperative Jahn–Teller-type lattice distortion in the CO state appears to be the largest at (or near) $x=0.75$ where the CO state is found to be very stable.[10] Moreover, it was observed that, in the CO state, there is a crossover of the Jahn–Teller vibration mode from Q_2 to Q_3 near $x=0.75$, which induces crossovers of the crystal structure from tetragonally compressed to tetragonally elongated orthorhombic, and of the magnetic structure from CE type to C type near $x=0.75$.[11] For $x>0.75$, both the Jahn–Teller distortion and the stability of CO state decrease with increasing doping level, and the magnetic structure is almost C type consistent with the Q_3-mode Jahn–Teller distortion. These features demonstrate the very important role of the cooperative Jahn–Teller effect in the CO state, and that the anomalies in the charge, spin, lattice, and orbital degree of freedoms at (or near) $x=6/8$ is one of the most important anomalies besides those observed at $x=$N/8 ($N=1, 3, 4, 5, 7$) for $La_{1-x}Ca_xMnO_3$. To get more insight into the CO state, it is very important to get more comprehensive understanding of the relationship among the spin, charge, lattice, orbital degree of freedoms, and the cooperative Jahn–Teller effect.

Internal friction and modulus measurements are nondestructive and very sensitive tools in studying microscopic relaxation processes and structural phase transitions in materials. It has been successfully employed to study the phase transitions, especially the Jahn–Teller effect in perovskite-type manganites.[12–14] In this article, we studied the relationship between the cooperative Jahn–Teller effect and the spin, charge, lattice, and orbital degree of freedoms by measurements of the transport, magnetic, specific heat, internal friction, and shear modulus in the charge ordering $La_{0.25}Ca_{0.75}MnO_3$.

II. EXPERIMENTAL DETAILS

The polycrystalline $La_{0.25}Ca_{0.75}MnO_3$ sample was synthesized via a coprecipitation method. Resistivity $\rho(T)$ was measured using a standard four-probe technique at tempera-

a)Author to whom correspondence should be addressed; electronic mail: lixg@ustc.edu.cn

Downloaded 07 Oct 2010 to 140.114.136.38. Redistribution subject to AIP license or copyright; see http://jap.aip.org/about/rights_and_permissions

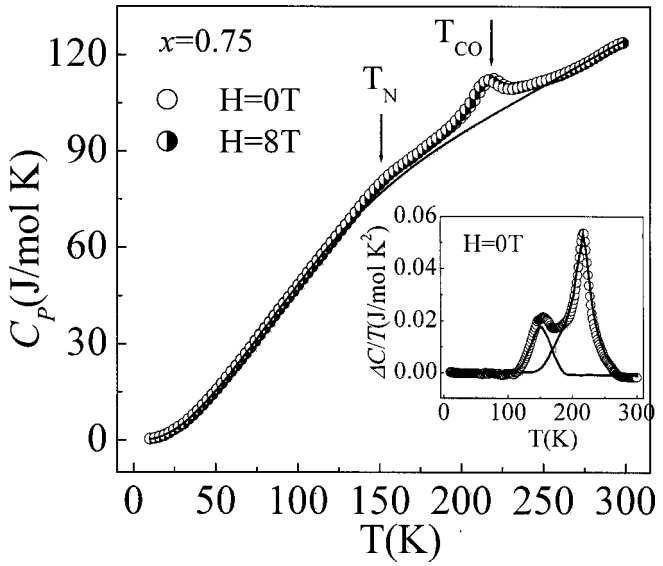

FIG. 1. Temperature dependence of the total specific heat C_P under $H=0$ and 8 T for $La_{0.25}Ca_{0.75}MnO_3$. The solid line represents the phonon contribution C_{phonon} to C_P. The inset is the $\Delta C/T$ vs T curve for $H=0$ T.

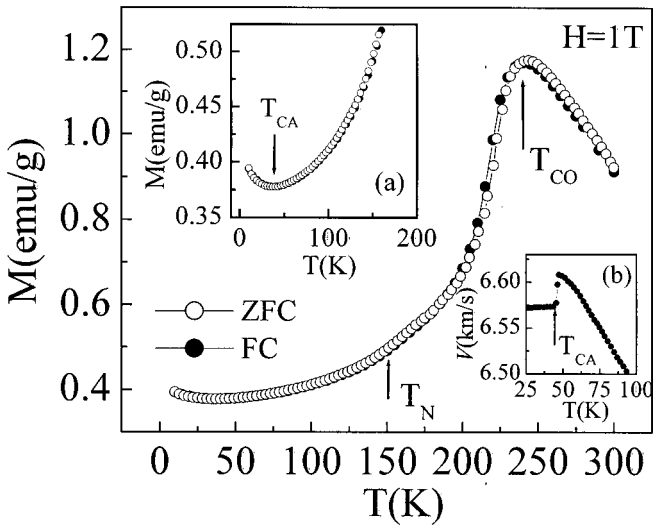

FIG. 2. Temperature dependence of the zero-field cooled and field-cooled magnetization for $La_{0.25}Ca_{0.75}MnO_3$. Inset (a) is the expanded view of the magnetization between 10 and 160 K. Inset (b) is the temperature dependence of the longitudinal ultrasound for $La_{0.25}Ca_{0.75}MnO_3$ measured with 10 MHz frequency.

tures from 4.2 to 300 K in magnetic fields up to 14 T. Zero-field cooled (ZFC) and field-cooled (FC) magnetization was measured using a commercial superconducting quantum interference device magnetometer at temperatures from 10 to 300 K at a field of 1 T. Specific heat was measured using a Quantum Design physical property measurement system magnetometer from 10 to 300 K at zero magnetic field and a magnetic field of 8 T. Low-frequency internal friction (Q^{-1}) and shear modulus *(G)* were measured on a multi-functional internal friction apparatus using the forced-vibration method with five different vibration frequencies of 0.1, 0.72, 1.00, 1.88 and 5.11 Hz during the warm-up from 120 to 475 K at the heating rate of 2.0 °C/min. The longitudinal ultrasound was measured using the Matec-7700 series ultrasonic equipment (Matec Instrument Companies) using a pulse-echo-overlap technique.

III. RESULTS AND DISCUSSION

Figure 1 shows the temperature dependence of the specific heat C_P under zero magnetic field and a magnetic field of $H=8$ T for $La_{0.25}Ca_{0.75}MnO_3$. The $\Delta C/T$ vs T curve for $H=0$ T is also shown in the inset of Fig. 1. According to Dulong–Petit's law, the limiting C_P at high temperature (e.g., 300 K) for a system containing r atoms per molecules is about $3rR$ J/mol K, where R is a gas constant.[15] For the $La_{0.25}Ca_{0.75}MnO_3$ compound with five atoms the calculated C_P is 124.7 J/mol K. The C_P(300 K) observed in our experiment is 123.8 J/mol K, which is 99.3% of the theoretically calculated value, indicating good date of C_P and quality of the sample. With decreasing temperature from 300 K a prominent jump of the specific heat is observed around T_{CO}. It is reasonable to attribute this large change of C_P to the entropy change due to the establishment of charge and orbital orderings as well as the simultaneously associated large changes of the lattice parameters.[10] With further decrease of temperature the C_P vs T curve shows a discernable change in slope around 152 K, which is very similar to those observed in charge-ordered $Pr_{1-x}Ca_xMnO_3$ ($x=0.37$, 0.4).[16–18] It should be noted here that neutron diffraction measurements on charge ordering manganites have shown that the long-range antiferromagnetic (AFM) ordering temperature T_N is usually much lower than T_{CO} (e.g., $T_{\text{CO}}=230$ K, $T_N=160$ K for $Pr_{0.63}Ca_{0.37}MnO_3$;[18] $T_{\text{CO}}=260$ K, $T_N=160$ K for $La_{0.35}Ca_{0.65}MnO_3$).[19] The small change of C_P around 152 K, therefore, can be mainly due to the formation of long-range AFM ordering for Mn ions since there is no evident change of the lattice parameters around this temperature.[10] After subtracting off a smooth background as the phonon contribution C_{phonon} to C_P, which is estimated by fitting a fifth-order polynomial to the C_P vs T curve at temperatures well away from T_N and T_{CO},[16] two partial overlapped peaks in $\Delta C/T = 0.058$ J/mol K^2 at T_{CO} and $\Delta C/T=0.018$ J/mol K^2 at T_N are visible. This two peaks can be decomposed into two individual peaks as shown by the solid line in the inset of Fig. 1. By numerically integrating the area under corresponding peaks, one can obtain the entropy change (ΔS) around T_{CO} and T_N. The calculated $\Delta S(T_{\text{CO}})$ and $\Delta S(T_{\text{N}})$ are about 2.32 J/mol K and 0.67 J/mol K, respectively. These values are in line with previous reports on similar materials. For example, $\Delta S(T_{\text{CO}})\approx 2$ J/mol K, $\Delta S(T_N)\approx 0.6$ J/mol K for charge-ordered $Pr_{0.6}Ca_{0.4}MnO_3$,[16] and $\Delta S(T_{\text{CO}})\approx 2.5$ J/mol K for charge-ordered $Y_{0.5}Ca_{0.5}MnO_3$.[20] We note that the specific heat peak near T_{CO} shifts slightly to a lower temperature by about 3 K upon the application of a magnetic field of 8 T, whereas the knee around 152 K remains unchanged, which reflects the very stable nature of the long-range AFM ordering for $T<T_N$.

In Fig. 2 we present the temperature dependence of the zero-field cooled (ZFC) and field-cooled (FC) magnetization for $La_{0.25}Ca_{0.75}MnO_3$. Both the ZFC and FC magnetizations increase with decreasing temperature from room tempera-

Downloaded 07 Oct 2010 to 140.114.136.38. Redistribution subject to AIP license or copyright; see http://jap.aip.org/about/rights_and_permissions

ture, and display maxima at T_{CO}. As the temperature is further cooled, the magnetization decreases rapidly, signaling the development of charge-ordered state. This magnetization peak can be understood in this picture: at high temperatures, the hopping of the e_g electrons between Mn^{3+} and Mn^{4+} ions induces a weak ferromagnetic spin correlation (The maximal magnetization at $H=1$ T is only 1.17 emu/g or 0.035 μ_B per Mn site). When the temperature is cooled below T_{CO}, there forms a kind of short-range AFM ordering for $T_N<T<T_{CO}$. In fact, just below T_{CO} fluctuations of orbital orientation are presented because of thermal activation. With decreasing temperature from T_{CO} the thermal activated fluctuations of the orbital orientation gradually decrease, and hence the $3d_{z^2-r^2}$ orbital orientation of Mn^{3+} ions becomes increasingly ordered along the *c* axis, causing a decrease of the magnetization because this orbital configuration can cause AFM ordering of the Mn ions as theoretically predicted.[21] When the temperature is lowered below T_N, the fluctuations of the orbital orientation are almost suppressed, and stable long-range $3d_{z^2-r^2}$ orbital ordering is established, causing the establishment of long-range AFM ordering with C-type magnetic structure. We note here that the neutron diffraction measurements on similar charge-ordered $La_{0.35}Ca_{0.65}MnO_3$ ($T_{CO}=260$ K) have shown that the long-range AFM ordering is not established until $T_N=160$ K.[19]

Another anomaly is the upturn of the magnetization near T_{CA} ($\approx$42 K) for both ZFC and FC cases. For a clear view, the expanded view of the ZFC and FC *M-T* curves near T_{CA} are shown in the inset (a) of Fig. 2. The upturn of magnetization for both ZFC and FC cases suggests that there, very possibly, develops partial spin canting in the matrix of long-range AFM ordering background, which is consistent with the fact that the ultrasound softens slightly near T_{CA} [see inset (b) of Fig. 2]. A similar small softening of ultrasound has been observed at about 48 K in $La_{0.67}Sr_{0.33}Mn_{0.87}Fe_{0.13}O_3$, and was attributed to the formation of magnetic spin-glass state.[22]

Figure 3 shows the temperature dependence of the resistivity under zero magnetic field ($H=0$ T) and a magnetic field of $H=14$ T for $La_{0.25}Ca_{0.75}MnO_3$. The resistivity for both $H=0$ and 14 T shows semiconductive behavior over the entire temperature range. Nevertheless, a conspicuous increase in the resistivity was observed near T_{CO}, characterizing the onset of the localization of the charge carriers onto specific lattice sites within the MnO_2 plane (i.e., charge ordering). We note that the resistivity for $H=14$ T remains almost the same as that for $H=0$ T over the entire temperature range, which suggests the very stable nature of the CO state for $La_{0.25}Ca_{0.75}MnO_3$. For perovskite-type manganese oxides, the electronic conducting mechanism in the CO state can usually be described by either the small polaron model or variable-range hopping (VRH) model.[19,23] The $\rho(T)$ behavior due to thermally activated nearest-neighbor hoppng of small polarons can be best fitted by the law:[24] $\rho \propto T\exp(E_a/K_BT)$, where K_B is the Boltzmann constant, and E_a is the activation energy. The $\rho(T)$ behavior due to variable-range hopping in a three-dimensional (3D) system can be best fitted by the law:[25] $\rho\propto \exp(T_0/T)^{1/4}$. The parameter T_0 is a characteristic temperature, and is related to the

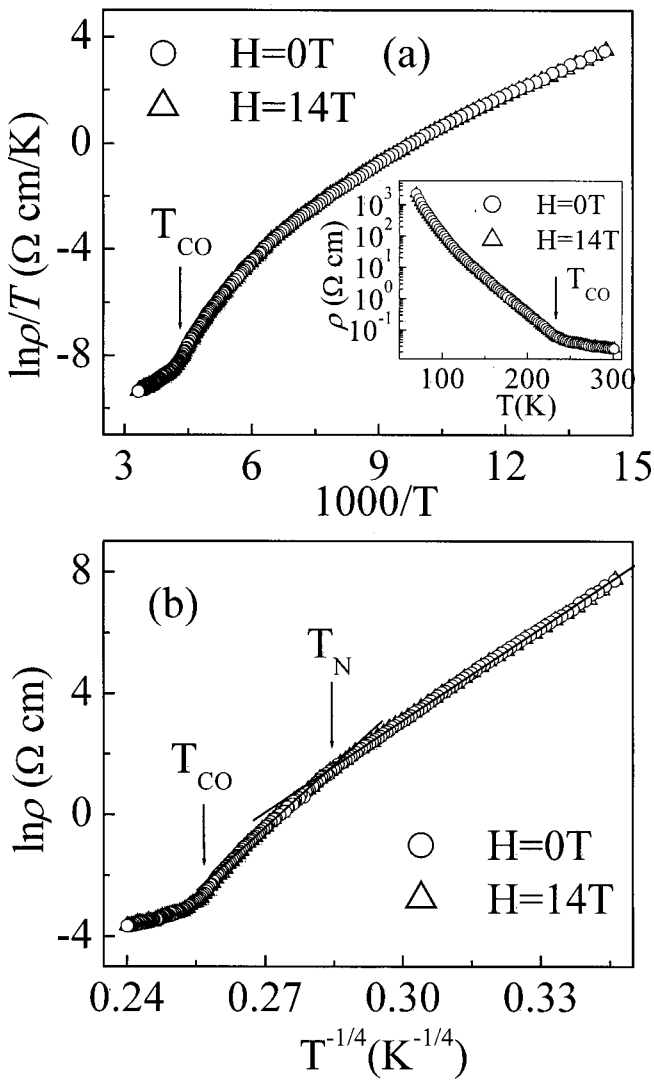

FIG. 3. (a) The $\ln\rho/T$ vs $1000/T$ curves under $H=0$ and 14 T for $La_{0.25}Ca_{0.75}MnO_3$. The inset in (a) is the temperature dependence of the resistivity for $H=0$ and 14 T. (b) the $\ln\rho$ vs $T^{-1/4}$ curves for $H=0$ and 14 T. The straight lines are linear fitted data for $T\leqslant T_N$ and $T_N<T<T_{CO}$, respectively.

density of states $N(E_F)$ at the Fermi level and the charge carrier localization length ξ as $K_BT_0\approx 18/[N(E_F)\xi^3]$ in 3D.[26] To find the conducting mechanism in the CO state, we fitted the resistivity data using the small polaron model and the VRH model. The $\rho(T)$ and linear fitted data according to the small polaron model and the VRH model are shown in Figs. 3(a) and 3(b), respectively. As seen in the inset of Fig. 3(a), no satisfactory linear $\ln(\rho/T)\sim 1000/T$ relationship is observed over the entire temperature range, indicating the electronic conduction in the CO state cannot be soundly described by the small polaron model. However, we found a good linear $\ln p\sim T^{-1/4}$ relationship in the CO state, but with a change in the slope (i.e., T_0) in the linear fitted data at about 150 K which is nearly coincident with the Néer temperature T_N for the long-range AFM ordering of the Mn ions for $La_{0.25}Ca_{0.75}MnO_3$. This implies that the conduction in the CO state follows the VRH mechanism, and that there is a change in the localization length ξ, assuming a constant density of states $N(E_F)$ across T_N. The fit to the $\rho(T)$ data

Downloaded 07 Oct 2010 to 140.114.136.38. Redistribution subject to AIP license or copyright; see http://jap.aip.org/about/rights_and_permissions

using $\rho \propto \exp(T_0/T)^{1/4}$ gives $T_0 = 3.17 \times 10^8$ K for $T_N < T < T_{CO}$, and $T_0 = 1.07 \times 10^8$ K for $T \leqslant T_N$. By taking the value of ξ to be 4 Å,[23] about the distance between neighboring Mn atoms, for $T_N < T < T_{CO}$. The $N(E_F)$ is estimated to be about 1.02×10^{19} $eV^{-1}\,cm^{-3}$ for $T < T_{CO}$ for $La_{0.25}Ca_{0.75}MnO_3$. This value agrees with the estimation of Sarathy *et al.*[23] that the $N(E_F)$ generally lies between 10^{18} and 10^{20} $eV^{-1}\,cm^{-3}$ for charge-ordered $Pr_{0.6}Ca_{0.4}MnO_3$, and $R_{0.5}Ca_{0.5}MnO_3$ (R=Nd, Gd). Using $N(E_F) \approx 1.02 \times 10^{19}$ $eV^{-1}\,cm^{-3}$ for our case, the ξ for $T \leqslant T_N$ is estimated to be 5.7 Å. The increase of ξ (or equivalently a decrease of T_0) at about T_N suggests a decrease of the disorder of the system for $T < T_N$ since T_0 is a representative of the extent of the disorder in a system and is high for highly disordered materials. As discussed above, the AFM ordering for $T_N < T < T_{CO}$ can be viewed as a kind of short-range type. This kind of short-range AFM ordering increases the scattering of the charge carriers, leading to a smaller localization length ξ and a larger T_0 for $T_N < T < T_{CO}$. As the long-range AFM ordering is established below T_N, the spin scattering of the charge carriers is suppressed to some degree, causing an increase in the ξ. Note that a very similar change in T_0 was observed near T_N for $Y_{0.37}Pr_{0.63}Ba_2Cu_3O_7$, and was attributed to the reduced scattering of the charge carriers due to the AFM ordering of Cu^{2+} spins in the CuO_2 planes.[27]

We note here that our previous low temperature powder x-ray diffraction measurements[10] on $La_{0.25}Ca_{0.75}MnO_3$ have shown that, when the temperature is cooled below T_{CO} the orthorhombic lattice parameters *a* and *c* undergo drastic increase just below T_{CO} (≈230 K), and become almost saturated below 200 K. In contrast, the *b* axis decreases continuously until about T_N (≈152 K) where long-range AFM ordering starts to be established. These large changes of lattice parameters are obviously due to the development of cooperative Jahn–Teller effect (i.e., orbital ordering),[28] and moreover, demonstrate that the development of orbital ordering mainly occurs in the temperature range between T_N and T_{CO}. As discussed above, the main part of the drop of the magnetization also locates in this temperature region where long-range AFM ordering is not established. From these magnetic and lattice dynamics for $T_N < T < T_{CO}$, one can further confirm that the orbital ordering can more or less influence the establishment of the AFM ordering, and the short-range AFM ordering between T_N and T_{CO} is very probably due to the orbital ordering.

The above analysis indicate that the development of orbital ordering plays a very important role in determining the magnetic and lattice dynamic below T_{CO}. Since the orbital ordering is a consequence of cooperative Jahn–Teller effect which can be detected by the measurement of elastic modulus, we measured the temperature dependence of the shear modulus (G) and internal friction (Q^{-1}) at five different frequencies for $La_{0.25}Ca_{0.75}MnO_3$ in order to get more information about the orbital dynamics. The experimental results are shown in Fig. 4. With decreasing temperature from a high temperature (475 K) to T_{CO} the shear modulus softens conspicuously, and reaches its minimum of T_{CO}, indicating drastic instability of the lattice near T_{CO}. This instability of the lattice to a strain of a given symmetry as evidenced by

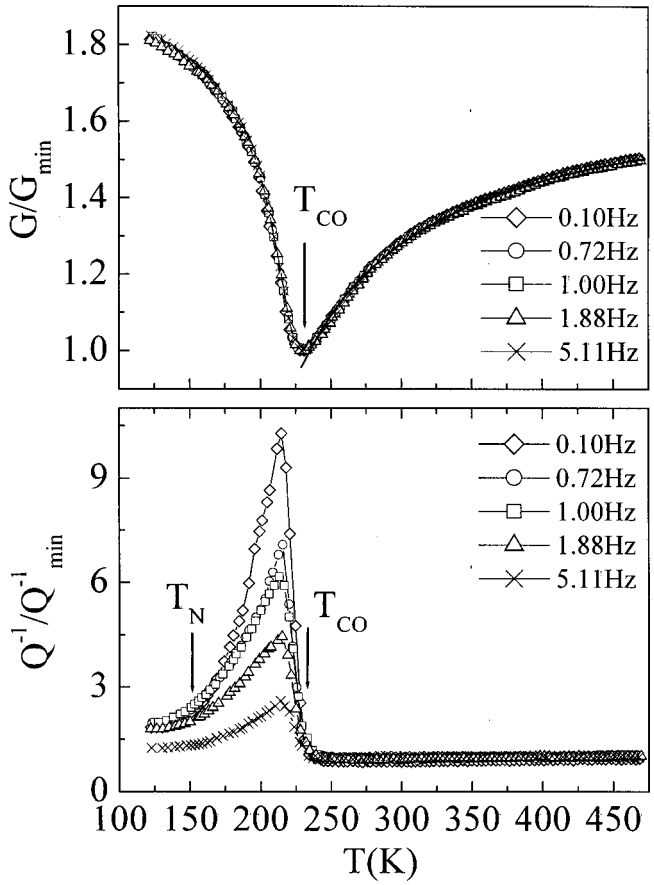

FIG. 4. Temperature dependence of the normalized shear modulus and internal friction measured with five different vibration frequencies for $La_{0.25}Ca_{0.75}MnO_3$. The sold line for $T > T_{CO}$ is a theoretical fit to the $G(T)$ data.

the drastic softening of the shear modulus is, in fact, a fundamental feature of cooperative Jahn–Teller phase transitions.[29] As the shear modulus reaches its minimum the lattice becomes unstable to strains of the corresponding symmetry and the crystal spontaneously changes to a more distorted lower symmetry phase (i.e., the distorted orthorhombic phase for $T < T_{CO}$). According to the Jahn–Teller phase transition theory, for $T > T_{CO}$, corresponding to the high temperature undistorted pseudo-cubic phase, the $G(T)$ behavior due to cooperative Jahn–Teller phase transition can be described by the equation[30] $G(T) = G(0)(T - (\lambda + \mu)/k_B)/(T - \lambda/k_B)$, here λ is the phonon exchange constant, μ is a measure of ion-strain coupling, and k_B is the Boltzmann constant. Following this equation, we fitted the $G(T)$ data for $T > T_{CO}$. It is seen that the fit is almost perfect with $(\lambda + \mu)/k_B = 175.5$ K and $\lambda/k_B = 132.3$ K. The ion-strain coupling energy which is the difference of $(\lambda + \mu)/k_B$ and λ/k_B[30,31] is 43.2 K. This value is comparable with those of $Pr_{1-x}Ca_xMnO_3$ ($x = 0.35,\ 0.5$).[30] It is worth pointing out here that the softening of G above T_{CO} and stiffening below T_{CO} are frequency independent. On the other hand, we note that the internal friction Q^{-1} increases steeply just below T_{CO}, which is coincident with the stiffening of shear modulus exactly. The internal friction peak height decreases with increasing frequencies, while the peak positions remain unchanged. These characters of Q^{-1}, to-

Downloaded 07 Oct 2010 to 140.114.136.38. Redistribution subject to AIP license or copyright; see http://jap.aip.org/about/rights_and_permissions

gether with the frequency independent stiffening of the shear moduli, indicate that the anomalies in G and Q^{-1} are mainly related to structural changes below T_{CO}, and no intrinsic relaxation process is involved in the CO transition.[32] As is known, in transition-metal oxides, the charge, spin, and orbital degree of freedoms, respectively, can cause elastic anomalies via the coupling between the lattice strain and the charges, the magnetic moments, and the quadrupolar moments, respectively.[33] Theoretical calculations and experimental results demonstrate that the coupling between the lattice strain and magnetic moments is much weaker than the coupling between the lattice strain and the charges or the orbital degree of freedoms. On the other hand, we note that the main part of the stiffening of the shear modulus and the internal friction peak mainly locate in the temperature region of $T_N < T < T_{CO}$ (see Fig. 4) where the orbital ordering develops rapidly. It seems that the shear modulus stiffening and internal friction peak mainly arise from the coupling between the lattice strain and the orbital degree of freedom.

IV. CONCLUSIONS

The transport, magnetic, specific heat, and lattice dynamics in charge-ordered $La_{0.25}Ca_{0.75}MnO_3$ have been studied. The development of cooperative Jahn–Teller effect (i.e., orbital ordering) leads to the internal friction peak, drastic stiffening of shear modulus, and a large decrease of the magnetization below T_{CO}. The AFM ordering between T_N and T_{CO} is short-range type, which was attributed to the thermally activated fluctuations of orbital orientation. The resistivity in the CO state follows Mott's VRH conduction $\rho \propto \exp(T_0/T)^{1/4}$ with a change in T_0 at about T_N which is very likely caused by the establishment of long-range AFM ordering of the Mn ions. A spin canting magnetic state was proposed to explain the upturn of the magnetization and the softening of the ultrasound at about $T_{CA} \approx 42$ K.

ACKNOWLEDGMENTS

This work was supported by the Chinese National Nature Science Fund, and the Ministry of Science and Technology of China.

[1] C. Martin, A. Maignan, M. Hervieu, and B. Raveau, Phys. Rev. B **60**, 12191 (1999).
[2] H. Fujishiro, T. Fukase, and M. Ikebe, J. Phys. Soc. Jpn. **67**, 2582 (1998).
[3] Y. Tokura, in *Colossal Magnetoresistance Oxides* (Gordon and Breach, Australia, 2000).
[4] S. Mori, C. H. Chen, and S.-W. Cheong, Nature (London) **392**, 473 (1998).
[5] A. P. Ramirez, P. Schiffer, S. W. Cheong, C. H. Chen, W. Bao, T. T. M. Palstra, P. L. Gammel, D. J. Bishop, and B. Zegarski, Phys. Rev. Lett. **76**, 3188 (1996).
[6] P. G. Radaelli, D. E. Cox, L. Capogna, S.-W. Cheong, and M. Marezio, Phys. Rev. B **59**, 14440 (1999).
[7] P. G. Radaelli, D. E. Cox, M. Marezio, S.-W. Cheong, P. E. Schiffer, and A. P. Ramirez, Phys. Rev. Lett. **75**, 4448 (1995).
[8] S. Mori, C. H. Chen, and S.-W. Cheong, Phys. Rev. Lett. **81**, 3972 (1998).
[9] E. O. Wollan and W. C. Koehler, Phys. Rev. **100**, 545 (1955).
[10] X. G. Li, R. K. Zheng, G. Li, H. D. Zhou, R. X. Huang, J. Q. Xie, and Z. D. Wang, Europhys. Lett. **60**, 670 (2002).
[11] R. K. Zheng, R. X. Huang, A. N. Tang, G. Li, X. G. Li, J. N. Wei, J. P. Shui, and Z. Yao, Appl. Phys. Lett. **81**, 3834 (2002).
[12] S. Seiro, H. R. Salva, M. Saint-Paul, A. A. Ghilarducci, P. Lejay, P. Monceau, M. Nunez-Regueiro, and A. Sulpice, J. Phys.: Condens. Matter **14**, 3973 (2002).
[13] F. Cordero, C. Castellano, R. Cantelli, and M. Ferretti, Phys. Rev. B **65**, 012403 (2002).
[14] T. W. Darling, A. Migliori, E. G. Moshopoulou, S. A. Trugman, J. J. Neumeier, J. L. Sarrao, A. R. Bishop, and J. D. Thompson, Phys. Rev. B **57**, 5093 (1998).
[15] E. S. R. Gopal, *Specific Heats at Low Temperatures* (Plenum, New York, 1966).
[16] M. R. Lees, O. A. Petrenko, G. Balakrishnan, and D. McK.Paul, Phys. Rev. B **59**, 1298 (1999).
[17] A. K. Raychaudhuri, A. Guha, I. Das, R. Rawat, and C. N. R. Rao, Phys. Rev. B **64**, 165111 (2001).
[18] V. Hardy, A. Wahl, C. Martin, and Ch. Simon, Phys. Rev. B **63**, 224403 (2001).
[19] M. R. Ibarra, J. M. DeTeresa, J. Blasco, P. A. Algarabel, C. Marquina, J. Garcia, and J. Stankiewicz, Phys. Rev. B **56**, 8252 (1997).
[20] A. Arulraj, R. Gundakaram, A. Biswas, N. Gayathri, A. K. Raychaudhuri, and C. N. R. Rao, J. Phys.: Condens. Matter **10**, 4447 (1998).
[21] D.I. Khomskii, Int. J. Mod. Phys. B **15**, 2665 (2001).
[22] C. F. Zhu, R. K. Zheng, J. H. Zhang, X. G. Li, J. R. Su, and Z. G. Zhu, J. Alloys Compd. **310**, 59 (2000).
[23] K. Vijaya Sarathy, S. Parashar, A. R. Raju, and C. N. R. Rao, Solid State Sci. **4**, 353 (2002).
[24] D. Emin and T. Holstein, Ann. Phys. (N.Y.) **53**, 439 (1969).
[25] N. F. Mott and E. A. Davis, *Electronic Processes in Non-Crystalline Solids*, 2nd ed. (Oxford University Press, New York, 1979).
[26] M. Viret, L. Ranno, and J. M. D. Coey, Phys. Rev. B **55**, 8067 (1997).
[27] W. Jiang, J. L. Peng, J. J. Hamilton, and R. L. Greene, Phys. Rev. B **49**, 690 (1994).
[28] P. G. Radaelli, D. E. Cox, M. Marezio, and S.-W. Cheong, Phys. Rev. B **55**, 3015 (1997).
[29] R. L. Melcher, in *Physical Acoustics*, edited by W. P. Mason (Academic, New York, 1976), Vol. 12, p. 1.
[30] H. Hazama, Y. Nemoto, T. Goto, Y. Tomioka, A. Asamitsu, and Y. Tokura, Phys. Rev. B **312,313**, 757 (2002).
[31] B. Lüthi and W. Rehwald, in *Structural Phase Transition I*, edited by K. A. Müller and H. Thomas, Topics in Current Physics Vol. 23 (Springer, New York, 1981).
[32] A. S. Nowick and B. S. Bery, in *Anelastic Relaxation in Crystalline Solids* (Academic, New York, 1972), p. 57.
[33] A. Imaduddin, K. Shimomura, Y. Nakanishi, Y. Kodama, K. Shibuya, H. Kanazawa, N. Yoshimoto, and M. Yoshizawa, Physica B **312,313**, 750 (2002).

Downloaded 07 Oct 2010 to 140.114.136.38. Redistribution subject to AIP license or copyright; see http://jap.aip.org/about/rights_and_permissions